

# PNIPAM nanogels and microgels at fluid interfaces

*Marcel Rey<sup>a,b,\*</sup>, Miguel-Angel Fernandez-Rodriguez<sup>c</sup>, Matthias Karg<sup>d</sup>,  
Lucio Isa<sup>c</sup> and Nicolas Vogel<sup>a,b,\*</sup>*

<sup>a</sup> Institute of Particle Technology (LFG), Friedrich-Alexander University Erlangen-

Nürnberg, Cauerstrasse 4, 91058 Erlangen, Germany

<sup>b</sup> Interdisciplinary Center for Functional Particle Systems (FPS), Friedrich-Alexander

University Erlangen-Nürnberg, Haberstrasse 9a, 91058 Erlangen, Germany

<sup>c</sup> Laboratory for Soft Materials and Interfaces, Department of Materials, ETH Zürich,

Vladimir-Prelog-Weg 5, 8093 Zürich, Switzerland

<sup>d</sup> Institut für Physikalische Chemie I: Kolloide und Nanooptik, Heinrich-Heine-

Universität Düsseldorf, Universitätsstr. 1, D-40225 Düsseldorf, Germany

## Conspectus

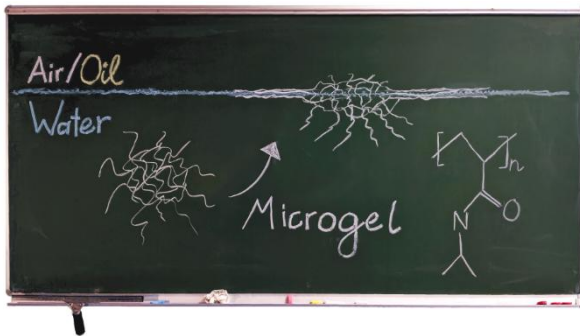
The confinement of colloidal particles at liquid interfaces offers many opportunities for materials design. Adsorption is driven by a reduction of the total free energy as the contact area between the two liquids is partially replaced by the particle. Since its first report in the early 20<sup>th</sup> century by Ramsden and Pickering, this phenomenon has attracted widespread attention. From an application point of view, particle-stabilized interfaces form emulsions and foams with superior stability. Liquid interfaces also effectively confine colloidal particles in two dimensions and therefore provide ideal model systems to fundamentally study particle interactions, dynamics and self-assembly. With progress in the synthesis of nanomaterials, more and more complex and functional particles are available for such studies.

In this review, we focus on poly(*N*-isopropylacrylamide) nanogels and microgels. These are cross-linked polymeric particles that swell and soften by uptaking large amounts of water. The incorporated water can be partially expelled, causing a volume phase transition into a collapsed state when the temperature is increased above approx. 32°C.

Soft microgels adsorbed to liquid interfaces significantly deform under the influence of interfacial tension and assume cross-sections exceeding their bulk dimensions. In particular, a pronounced corona forms around the microgel core, which is formed by the dangling chains at the microgel periphery. These polymer chains expand at the interface and strongly affect the inter-particle interactions. The particle deformability therefore leads to a significantly more complex interfacial phase behavior that provides a rich playground to explore structure formation processes.

We first discuss the characteristic “fried-egg” or core-corona morphology of individual microgels adsorbed to a liquid interface and comment on the dependence of this interfacial morphology on their physico-chemical properties. We introduce different theoretical models to describe their interfacial morphology. In a second part, we introduce how ensembles of

microgels interact and self-assemble at liquid interfaces. The core-corona morphology and the possibility to force these elements into overlap upon compression results in a complex phase behavior with a phase transition between microgels with extended and collapsed coronae. We discuss the influence of the internal particle architecture, also including core-shell microgels with rigid cores, on the phase behavior. Finally, we present new routes for the realization of more complex structures, resulting from multiple deposition protocols and from engineering the interaction potential of the individual particles.



## Introduction

The ability of colloidal particles to adsorb to liquid interfaces is of fundamental importance for a range of scientific disciplines and directly impacts technological applications,<sup>1</sup> for example by imparting mechanical and kinetic stability to emulsions or foams.<sup>2</sup> The first reports on this phenomenon date back to the early 20<sup>th</sup> century with the work by Ramsden and Pickering on emulsions.<sup>3,4</sup> In these emulsions, often called Pickering emulsions, droplets are stabilized by a coating of solid particles on their surfaces. In 1980, Pieranski developed a simplistic model to understand why particles adsorb at liquid interfaces instead of being dispersed in the bulk of either phase.<sup>5</sup> He calculated the change in contributions of surface energy upon moving a spherical colloidal particle across a fluid interface. Crucially, for a uniform spherical particle, a unique energy minimum develops, whose depth and position depends on the interfacial tension, the particle size and its contact angle. Given the typical values of interfacial tensions for standard water-oil interfaces  $\sim 10^1$ - $10^2$  mN/m, the energy required for micron-sized particles to escape the interface can easily exceed the thermal energy by a factor of  $10^6$ . Therefore, liquid interfaces very effectively confine colloidal particles in two dimensions, a fact that provides the kinetic stabilization observed in Pickering emulsions. Moreover, confinement allows for studies of the particles' interactions and dynamics within the interface.<sup>1,5,6</sup> The ability to resolve individual particles directly with an optical microscope, paired with well-understood and controllable interaction potentials, renders colloidal particles trapped at interfaces ideal model systems for fundamental studies of self-assembly phenomena.<sup>7-9</sup>

The propensity to adsorb and be confined at fluid interfaces is retained by soft, deformable particles. In contrast to conventional, rigid particles, the coupling between particle elasticity, molecular architecture and interfacial effects enables a much richer palette of interfacial phenomena to be exploited in fundamental and applied studies alike. In this review, we focus

on soft poly-*N*-isopropylacrylamide (PNIPAM) microgels at fluid interfaces and discuss their morphology and self-assembly behavior at liquid interfaces in dependence of their physico-chemical properties. We further address the influence of the internal architecture and interaction potential in the case of microgels that possess a core-shell structure with rigid, inorganic cores. These core-shell microgels enable the formation of complex and hierarchical surface structures with functionalities that can be tailored by the choice of the core material and size.

### **Microgels in bulk:**

Microgels are soft and deformable objects with an internal gel-like structure that typically possess dimensions in the colloidal size range.<sup>10</sup> When dispersed in a suitable solvent, microgels can swell to multiples of their dry diameter by an uptake of solvent. Microgels based on chemically crosslinked PNIPAM are the most extensively studied model system as they can be synthesized by precipitation polymerization with high control over size with low polydispersities (Figure 1).<sup>11,12</sup> Furthermore, PNIPAM microgels exhibit stimuli-responsive characteristics with a volume phase transition (VPT) from a highly swollen state to a partially collapsed state at a transition temperature of approximately 32°C.<sup>13–15</sup> This VPT is attributed to the lower critical solution temperature (LCST) of the PNIPAM polymer in water. At this temperature, water is expelled from the macromolecule and the non-polar groups start to aggregate. Both swelling behavior and phase transition can be tailored at a molecular level by the incorporation of comonomers.<sup>16</sup> For example, the ionic comonomer methacrylic acid (MAA) induces a pH-responsiveness as the microgels swell more in the deprotonated state at high pH due to an additional osmotic pressure contribution as compared to the protonated state at low pH.<sup>16,17</sup>

Typical PNIPAM microgels that are chemically crosslinked by *N,N'*-methylenebis(acrylamide) (BIS) show a pronounced crosslinking gradient from the center towards the outside. This gradient is related to the different reactivities of the monomer and the crosslinker.<sup>18</sup> Small angle neutron scattering experiments showed that such purely organic microgels can be described by a “core-shell” model in bulk, with a comparably harder core region with higher crosslinking density and a soft corona with dangling chains.<sup>19</sup> The crosslinking gradient can be mitigated via the synthesis, for example by following a continuous feed strategy<sup>20</sup> or using miniemulsion polymerization.<sup>21</sup>

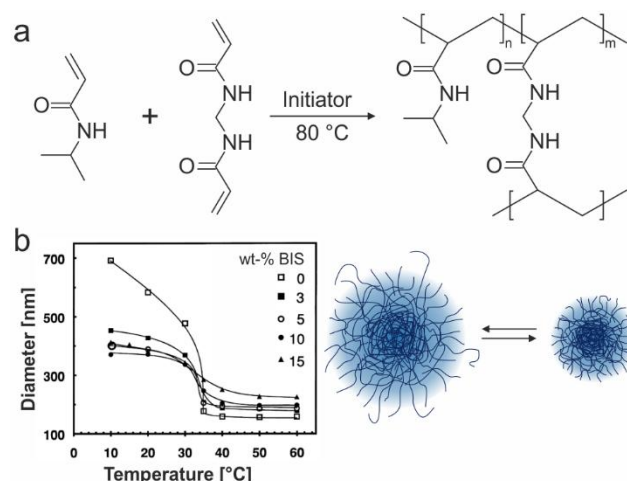


Figure 1: Chemical synthesis and stimuli-responsive behavior of PNIPAM microgels. a) The precipitation polymerization of *N*-isopropylacrylamide with *N,N'*-methylenebis(acrylamide) (BIS) crosslinker above the LCST of the PNIPAM polymer leads to the formation of crosslinked PNIPAM microgels. b) Hydrodynamic diameter versus temperature diagram for microgels with various crosslinking densities (BIS) showing the volume phase transition from an expanded to a collapsed state at 32 °C and an increase in swelling for lower crosslinking densities. Adapted with permission from ref. 15. Copyright 1993 Elsevier.

### Single soft microgels at interfaces:

PNIPAM microgels strongly adsorb to liquid interfaces and reduce the interfacial energy between the air or oil phase and the water phase, similarly to hard particles.<sup>14</sup> In contrast to hard particles, however, microgels are soft and can deform upon adsorption, which leads to two major characteristics of their interfacial shape: 1) due to the surface activity of PNIPAM,

the portion of a microgel that is in contact with the interface stretches out, occupying a larger area to reduce the free-energy of the interface until this energy gain is balanced by internal elasticity, and 2) the microgel protrudes into the two fluids according to their respective affinities. Typically, this gives rise to an asymmetric shape, as the microgel portion immersed in water is swollen, while the portion protruding towards air/oil is (partly) collapsed. The extent of the in-plane deformation and of the asymmetry across the interface are a function of the architecture of the microgel and of the nature of the fluid phases.

The deformation of the microgels can be for instance visualized using fluorescence microscopy (Figure 2a). In this case, for relatively large microgels with low crosslinking density, the microgel cross-sectional area increased by a factor 10 at the air/water interface.<sup>22</sup> The morphology of microgels at alkane/water interfaces can also be directly observed by cryo-scanning electron microscopy (cryo-SEM)<sup>23,24</sup> or by freeze-fracture shadow casting cryo-SEM (FreSCa).<sup>25-28</sup> These techniques revealed the existence of a “fried-egg” morphology, which results from the higher deformability of the loosely crosslinked corona compared to the higher crosslinked core region for both flat interfaces of water/oil (Figure 2b-c) and curved interfaces in emulsions (Figure 2d,e).<sup>23-28</sup> In a typical FreSCa experiment, shown in Figure 2b, the oil is removed after fracturing and the portion protruding towards the oil phase is exposed, from which the 3D shape of the can microgel be partly reconstructed. In this case, a 1.5-fold increase of the particle diameter at the interface and a weak protrusion into the oil were observed. In the case of fracture perpendicular to the interface, Fig. 2c, the microgels can to be visualized from the side and the part exposed to the water phase is revealed. These two experiments proved that microgels stretch at the interface while their portion immersed in oil collapses (both visible in Fig. 2b and 2c) and the portion immersed in water stays hydrated (in Fig. 2c). *In-situ* small angle neutron reflectivity of PNIPAM nanogels at air/water interfaces additionally revealed that the corona consists of a few nanometers thin film of polymer with low water content, preventing core-core contact between neighboring

microgels (Figure 2f),<sup>29</sup> as also shown by cryo-SEM in the emulsions shown in Figure 2d,e.<sup>23</sup> In addition, these experiments revealed that the core elastically deforms under the effect of surface tension but remains swollen, while the remaining dangling chains that are not part of the corona are hydrated in water and collapsed in air.<sup>29</sup>

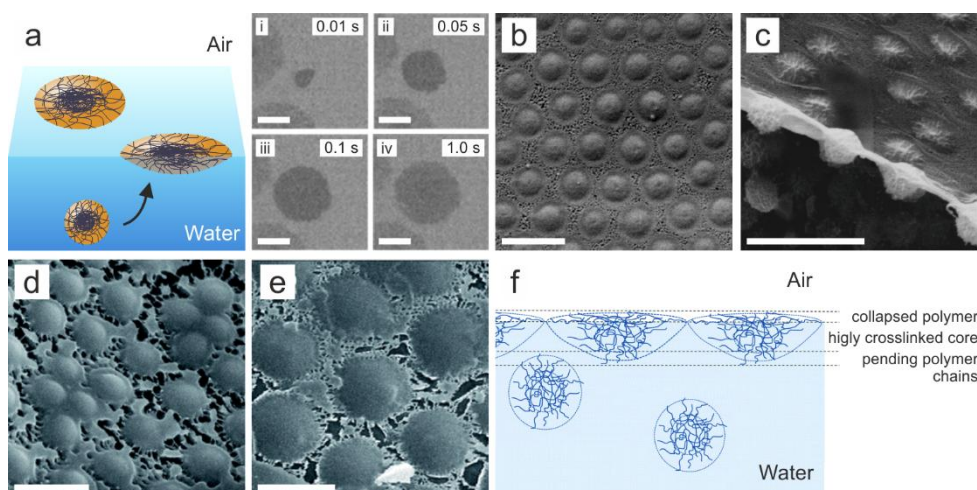


Figure 2: Spreading and morphology of PNIPAM microgels adsorbed to air/water or oil/water interfaces. a) Fluorescence microscopy of PNIPAM microgels (diameter: 6.3  $\mu\text{m}$ , 1.4 mol-% BIS) adsorbed to the air/water interface. During adsorption they laterally expand by a factor of 10. Adapted with permission from ref. 22. Copyright 2011 the Royal Society of Chemistry. b,c) FreSCa SEM images of PNIPAM microgels adsorbed to the oil/water interface: b) top view of the oil/water interface. Adapted with permission from ref. 25. Copyright 2012 American Chemical Society. c) Side view across the interface. Adapted with permission from ref. 27. Copyright 2015 the Royal Society of Chemistry. d,e) Cryo SEM images of oil/water emulsions stabilized by PNIPAM microgels. Adapted with permission from ref. 23. Copyright 2011 the Royal Society of Chemistry. f) Model of PNIPAM nanogels adsorbed to the air/water interface based on neutron reflectivity. Adapted with permission from ref. 29. Copyright 2016 the Royal Society of Chemistry. a) Scale bar: 10  $\mu\text{m}$ . b-e) Scale bar: 1  $\mu\text{m}$ .

The deformation of the microgels at the interface is restricted by their bulk elasticity. It can be modeled as an interplay between the reduction of interfacial energy between two immiscible liquids and the elastocapillary length  $L = \gamma_s/E$  of the microgel, comparing the surface tension of the solid  $\gamma_s$  to its Young's modulus  $E$ .<sup>27</sup> When the particle radius is large with respect to the elastocapillary length, it can be considered as effectively rigid, only showing slight deformations near the contact line. In contrast, for small particle dimensions, the particle can effectively be considered a liquid (Figure 3a). The spreading is sensitive to differences in interfacial energy between the two immiscible liquids. The model predicts that smaller and



less-crosslinked (softer) microgels deform more at the interface. These calculations describe well the spreading and flattening of the microgel core observed experimentally.<sup>22,25</sup> However, the formation of a corona is not considered in this approach as the model assumes homogeneous entities made of fluids or linear-elastic solids.

To account for the corona, dissipative particle dynamics was used to simulate the behavior of microgels at interfaces.<sup>30</sup> Similar to the elasticity-based model, the microgel spreading depends on the interfacial energy between the two immiscible liquids. In addition to the deformation of the microgel core, the chain-based model reproduces the formation of a small, thin corona consisting of stretched dangling chains adsorbed to the interface (Figure 3b). For large enough interfacial energies (here:  $\gamma_{AB}=60$ ), the model reproduces the experimentally observed "fried-egg" like structure reasonably well (see Fig. 2b-d). To take into account for network inhomogeneities present in synthesized microgels, a randomized crosslinking structure was used. This non-uniform distribution of crosslinking points leads to a distribution of different dangling chain lengths.<sup>31</sup> These dangling chains affect the morphology of the microgel at the interface as they stretch out and form a thin corona to maximize the interfacial coverage (Figure 3c).

In order to realize a more realistic molecular picture that captures the crosslinking gradient of PNIPAM microgels produced by standard one-pot synthesis,<sup>19</sup> numerical models are produced by an *in silico* assembly of tetravalent (crosslinker) and bivalent (monomer) patchy beads into microgels.<sup>32,33</sup> Such models show quantitative agreement of the internal structure with experimental results obtained by small-angle X-ray scattering experiments.<sup>32,33</sup> When adsorbed at an oil/water interface such model microgels accurately reproduce the characteristic "fried-egg" morphology observed in experiment (Figure 3d) as well as the crosslinking density-dependent protrusion of the microgels into the oil phase, by an appropriate choice of the interaction parameters between the monomers and the two fluids.<sup>28</sup>

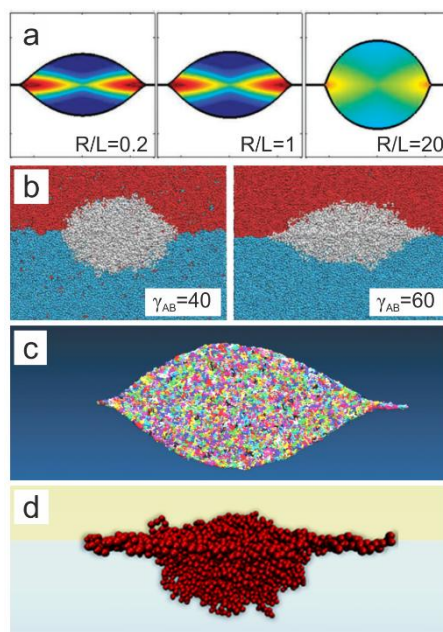


Figure 3: Models and simulations used to explain the behavior of microgels adsorbed to a liquid interface. a) Calculated equilibrium shape for homogenous microgels adsorbed to a liquid interface in dependence of the ratio  $R/L$ , between their radius and the elastocapillary length. Adapted with permission from ref. 27. Copyright 2015 the Royal Society of Chemistry. b) Dissipative particle dynamic simulation of microgels deformation in dependence of the interfacial energy ( $\gamma_{AB}$ ). Adapted with permission from ref. 30. Copyright 2016 the Royal Society of Chemistry. c) Molecular dynamic simulation of a microgel with random crosslinking distribution. Adapted with permission from ref. 31. Copyright 2015 the Royal Society of Chemistry. d) Molecular dynamics simulation of microgels synthesized *in silico* including a crosslinking gradient showing the characteristic “fried-egg” morphology and anisotropic protrusion characteristics. Adapted with permission from ref. 28. Copyright 2019 American Chemical Society.

### Self-assembly of PNIPAM microgels at fluid interfaces

After analyzing the morphology of individual PNIPAM microgels adsorbed at liquid interfaces, we discuss their self-assembly behavior under two-dimensional interfacial confinement. The small size of the microgels, paired with a low refractive index contrast due to the large water content, often prevents a direct observation *via* optical microscopy. The collective organization at the interface can thus be either investigated by *in-situ* techniques such as FreSCa<sup>25–28</sup> and cryo-SEM of emulsion droplets<sup>34</sup> or *ex situ* by transferring the interfacial microgel layer onto a solid substrate, followed by characterization with SEM or atomic force microscopy (AFM).<sup>26,35–38</sup> While the *in-situ* techniques allow a direct

visualization of a nearly undisturbed interface, they rely on the spontaneous adsorption of the microgels from the water phase to the liquid interface, making it difficult to control and manipulate the packing density at the interface. In contrast, the packing density can be conveniently adjusted with a Langmuir-Blodgett trough, while simultaneously determining interfacial properties such as the interfacial tension of the system. For the characterization, however, this interfacial layer structure has to be transferred to a solid substrate, and may therefore be affected by drying artefacts. In the simultaneous compression and deposition technique, the compression of the interfacial microgel layer and the deposition onto a solid substrate is synchronized (Figure 4a). This technique encodes the surface pressure in the trough to a precise position of the solid substrate and therefore allows for the investigation of the complete evolution of the phase behavior on a solid substrate within one experiment (Figure 4b,c).<sup>26,35,37,39</sup>

Langmuir-Blodgett depositions of poly(*N*-isopropylacrylamide-co-acrylic acid) microgels revealed five distinct phases (Figure 4a).<sup>36,37</sup> At low surface pressure ( $< 1$  mN/m), when the microgel concentration is insufficient to fully cover the interface, the microgels are either distributed in a “liquid”-like state (Figure 4b) or forming clusters due to capillary attraction.<sup>24,36</sup> With increasing microgel concentration at the interface, the microgels start crystallizing into an hexagonal structure, with microgels in corona-corona contact. In this phase, the cores are substantially separated from each other as the coronae act as spacers between them (Figure 4b,c). Because the corona is extremely thin and not visible in AFM height images or by SEM, this phase resembles a non-close packed structure. Further compression leads to a decrease in interparticle distance of the hexagonal corona-corona contact arrangement (Figure 4c) until the microgels undergo a well-defined solid-solid phase transition (Figure 4c). A new hexagonal phase with microgels in core-core contact nucleates in the corona-corona contact phase, with clear regions of coexistence between the two phases.<sup>35</sup> Even though this phase transition was characterized *ex situ*, where capillary forces

during drying may alter the assembly behavior, the same phases and phase transitions can also be observed in cryo-SEM images (Figure 4d), indicating that the phase transition is not a drying artefact but occurs at the liquid interface.

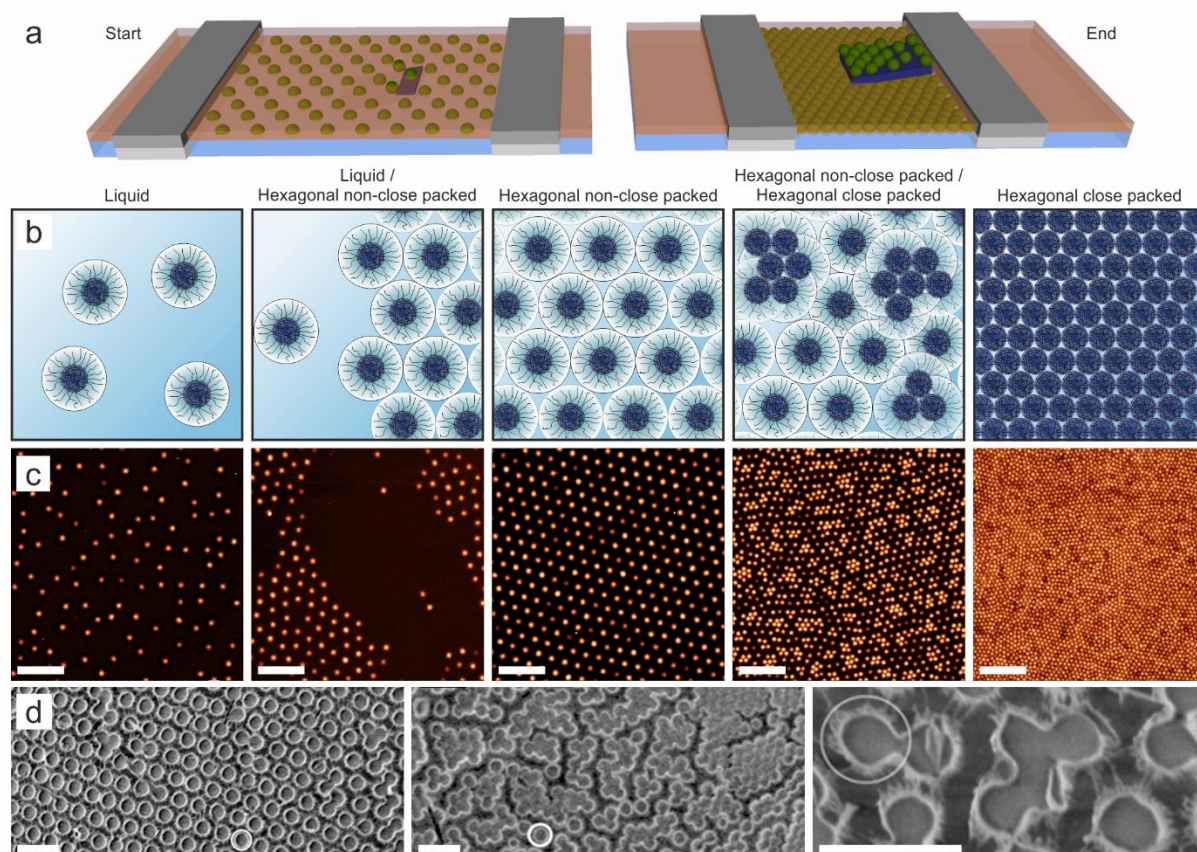


Figure 4: Microgel self-assembly at liquid interfaces. a) Schematic illustration of the simultaneous compression and deposition method often used to characterize the phase behavior of microgels. b,c) Schematic representation (b) and corresponding AFM images (c) of the phase behavior of PNIPAM-AA microgels confined at the oil/water interface including an isostructural solid-solid phase transition from a hexagonal non-close packed phase to a hexagonal close packed phase. Adapted with permission from ref. 37. Copyright 2016 the Royal Society of Chemistry. d) *In-situ* cryo-SEM images of oil/water emulsions showing the same phases and phase transitions. Adapted with permission from ref. 34. Copyright 2011 American Chemical Society. All scale bars: 2  $\mu\text{m}$ .

### Physico-chemical parameters affecting the interfacial phase behavior:

The complex interfacial phase behavior of microgels arises from a combination of the microgels' macromolecule-, surfactant- and colloidal properties.<sup>14</sup> Knowledge of this interplay

and the influence of the different physico-chemical properties, discussed in this section, is therefore crucial to understand, predict and tailor the interfacial properties of microgels.

**Electrostatic Repulsion:** The influence of electrostatic repulsion on the spreading and self-assembly behavior of PNIPAM-co-AAc microgels was investigated by controlling the charge density of the microgels by changing the pH of the water subphase.<sup>17,38</sup> Even though one might intuitively expect an increased repulsion when the microgels possess a charge, charged and uncharged microgels showed a similar core-corona morphology and dimensions in the FreSCa cryo-SEM images, as well as a similar shape of the normalized compression curve (Figure 5a).<sup>17,38</sup> Surprisingly, the compression of more charged microgel monolayers at oil/water interfaces revealed a softer response, demonstrating that the inclusion of charged moieties affects the swellability and the collective mechanical properties of the microgel corona.<sup>17,40</sup>

demonstrating that, differently from the case of hard colloidal particles, there is an interplay between electrostatic effects, swelling and collective mechanical properties.

**Size:** The influence of size on the interfacial properties was investigated using microgels synthesized with a range of different sizes.<sup>26</sup> Large microgels showed a clear core-corona morphology (Figure 5f), while small microgels had a fuzzy corona (Figure 5g). The difference in morphology also translated into differences in the interfacial phase behavior upon compression. While large microgels underwent a solid-solid phase transition, smaller microgels were continuously compressible at the liquid interface without exhibiting a phase transition. These experiments indicate that the surface-to-volume ratio may affect the morphology of the microgels at the interface. Since smaller microgels have more dangling chains per volume, they appear more “fuzzy” and behave as mechanically polydisperse soft disks, whereas the larger microgels have a more pronounced core-corona morphology.

Therefore, strictly speaking, the observed phenomenon is not a size effect, but an effect related to differences in internal structure found in larger and smaller microgels.

**Internal structure:** Apart from the crosslinking density that ultimately defines the swelling capacity and thus the softness of purely organic microgels, the internal structure is dominated by the pronounced crosslinking gradient<sup>18</sup> - with the exception of microgels with an ultra-low crosslinking density.<sup>41</sup> The softness and core-shell like structure have a strong impact on the phase behavior at interfaces. Softer microgels are able to withstand higher pressures before collapsing into core-core contact and show a more pronounced corona (Figure 5d,e).<sup>35,38</sup> Consequently, the onset of the phase transition is shifted to higher surface pressures for lower crosslinking densities (Figure 5b, squares) combined with an decreased height after drying (Figure 5c). Interestingly, very soft microgels (1 mol-% crosslinker in the studies) did not show any phase transitions.<sup>35,38</sup> Instead, the interparticle distance decreased continuously upon compression.

Recent work focused on microgels with a combination of small size and ultra-low crosslinking density.<sup>41</sup> While these show a particulate nature in bulk, when adsorbed to the oil/water interface, a more polymer-like behavior was found. Such microgels do not exhibit a core-shell structure and spread into flat discs with a uniform height of 1 nm (Figure 5h). Once the interface is fully covered with microgels, they formed a homogenous polymer film (Figure 5i). Upon compression, individual microgels were recognizable again (Figure 5j,k). These findings show that the internal molecular architecture of the microgels strongly affects the morphology and the phase behavior of microgels at liquid interfaces.



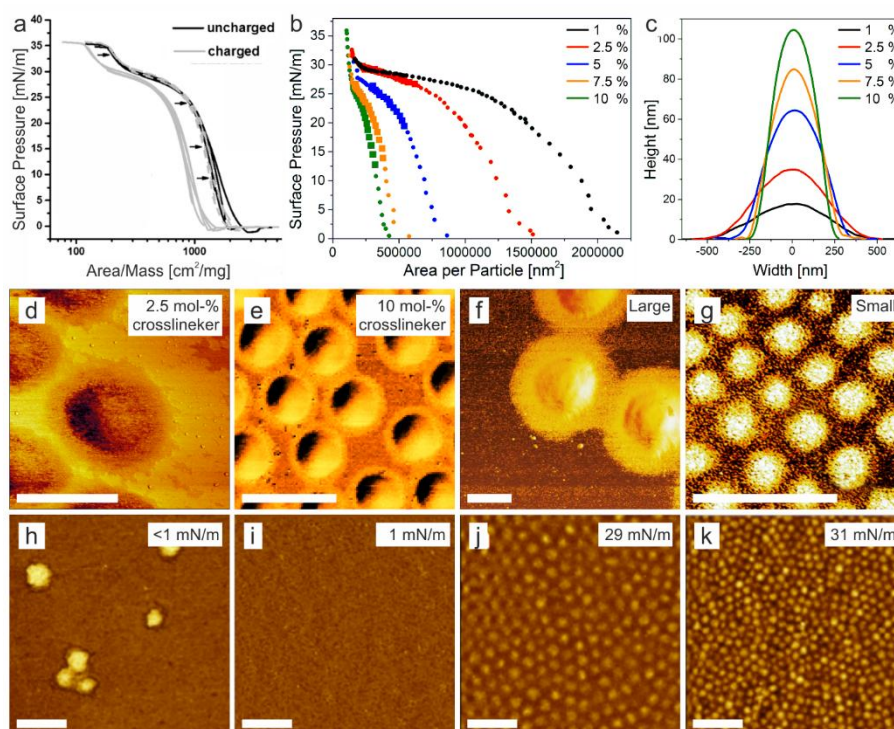


Figure 5: Effect of physico-chemical properties on the interfacial morphology and self-assembly behavior of PNIPAM microgels adsorbed at liquid interfaces. a) Charged and neutral PNIPAM-co-AA microgels show a similar normalized compression curve. Adapted with permission from ref. 17. Copyright 2014 Wiley-VCH. b-e) A lower crosslinking density leads to an increase in deformability of the microgels at the liquid interface, resulting in larger area per particle (b) combined with a lower height (c) and a more pronounced corona for 2.5 mol-% crosslinking density (d) compared to 10 mol-% crosslinking density (e). Reprinted with permission from ref. 35. Copyright 2017 the Royal Society of Chemistry. f,g) AFM phase images of large (f) and small microgels (g), showing differences in the structure of the corona. Adapted with permission from ref. 26. Copyright 2017 the Royal Society of Chemistry. h-k) AFM height images of ultra-low crosslinked small microgels spreading into flat discs (h) and form a homogenous polymer film at the interface (i), where the individual microgels are not recognizable. Only upon compression the particulate morphology of the microgels is visible again (j,k). Adapted with permission from ref. 41. Copyright 2019 Springer Nature. All scale bars: 1  $\mu\text{m}$ .

The extreme case of microgels with an internal density gradient are core-shell microgels that contain a rigid core. A typical model system are  $\text{SiO}_2$ -PNIPAM core-shell particles consisting of an incompressible silica core surrounded by a soft PNIPAM shell.<sup>42,43</sup> The stiff silica core leads to an increased protrusion into the oil phase and again a pronounced “fried-egg” like appearance (Figure 6a).<sup>39</sup> The non-deformable core further induces local deformations of the interface and therefore increases capillary attractions between the individual particles compared to conventional microgels. As a consequence, at low surface coverage such core-

shell particles form 2D aggregates with large voids instead of a uniform monolayer occupying the available space (Figure 6b-c).<sup>44,45</sup> Upon compression, these aggregates are continuously pushed together until a homogenous monolayer is formed (Figure 6d).<sup>44</sup> The core-shell microgels also undergo a solid-solid phase transition, however, with the onset of the phase transition shifted to lower surface pressures compared to conventional microgels (Figure 6e-g).<sup>39,46</sup> The increased refractive index contrast due to the inorganic cores produces structural coloration *via* grating diffraction, which enables an easy, visual determination of the phase transition region, where the order of the grating is disturbed by the nucleation of the close-packed phase (Figure 6f).<sup>46</sup> Regions with a homogeneous lattice before and after the phase transition appear iridescent, while a white color results from the disordered phase transition region. Similar to the case of conventional microgels, the interfacial phase behavior of the core-shell particles depends on the softness of the shell, i.e. the crosslinking density, as well as the crosslinker distribution. However, due to the rigid core another length scale becomes relevant: The core size with respect to the shell thickness. In particular, recent calculations showed that there exists a critical ratio between core size and shell thickness for which the microgel behaves as if the core was absent. This critical value is a weak function of the core size but crucially depends on the extent of shell stretching at the interface, which is determined by its architecture.<sup>47</sup> Thus, the phase behavior of core-shell microgels at interfaces is governed by the complex interplay between the core-to-shell size ratio and the internal shell morphology.<sup>39,46,47</sup>



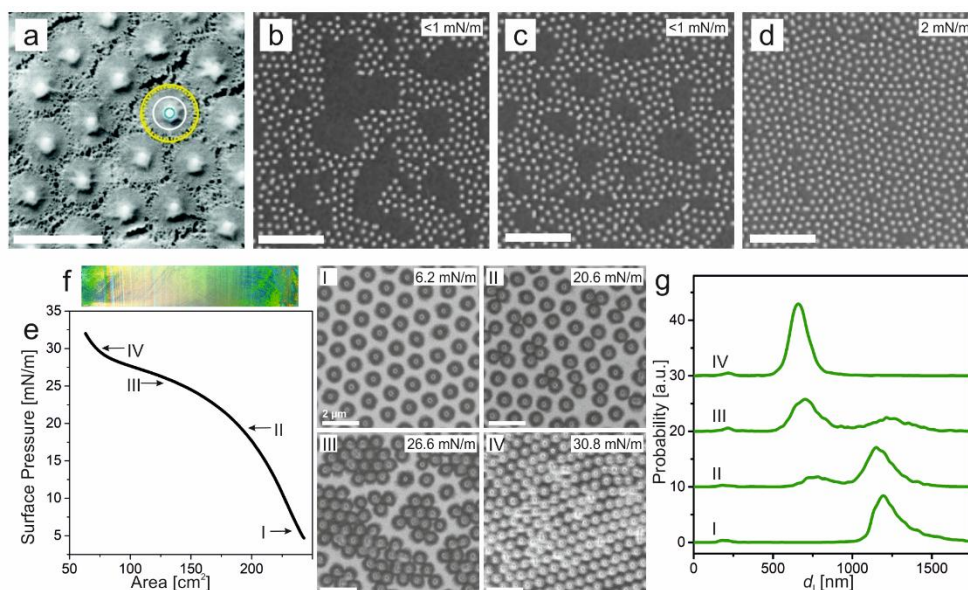


Figure 6: Influence of an inorganic core on the phase behavior of PNIPAM microgels at liquid interfaces. a) FreSCacryo-SEM image of  $\text{SiO}_2$ @PNIPAM core-shell particles displaying a pronounced “fried-egg” morphology. Scale bar. 1  $\mu\text{m}$ . Reprinted with permission.<sup>39</sup> Copyright 2016, the Royal Society of Chemistry. b-d)  $\text{SiO}_2$ @PNIPAM core-shell particles assemble into aggregates with voids at low packing density which are annealed upon compression. Adapted with permission from ref. 44. Copyright 2018 American Chemical Society. Scale bars: 10  $\mu\text{m}$ . e-g) Phase diagram of  $\text{SiO}_2$ @PNIPAM core-shell particles showing an isostructural solid-solid phase transition. e) Surface pressure - area curve with the corresponding photograph of the substrate (f) and SEM images of the phases shown in (I-IV). g) The interparticle distance distribution shows the coexistence of two phases during the transition. Reprinted with permission from ref. 46. Copyright 2018, American Chemical Society. Scale bars 2  $\mu\text{m}$ .

**Volume phase transition at the interface:** PNIPAM microgels can be used to form temperature-sensitive emulsions, which are stable at room temperature and can be destabilized by heating the emulsion above the volume phase transition temperature (VPTT).<sup>48–50</sup> Since the destabilization temperature coincides with the VPTT of the microgels, it was often attributed to a lateral shrinkage or desorption of the microgels from the liquid interface. However, two recent reports show that compared to the bulk behavior (Figure 1b), the temperature-dependent volume phase transition of a PNIPAM microgel adsorbed to an oil/water or air/water interface is strongly hindered.<sup>51,52</sup> The interparticle distance of such interfacial microgel assemblies remains unaffected by an increase in temperature (Figure 7a), and the diameter of the microgel cores only changes slightly (Figure 7b).<sup>51</sup> Furthermore, the characteristic “fried-egg” or core-corona morphology remained even at temperatures above

the temperature of the VPT, demonstrating that the polymer chains within the corona did not undergo a phase transition (Figure 7c-f). The swollen microgel core and dangling chains extending away from the interface into the bulk liquid exhibited a collapse in z-direction (Figure 7e,f). Together, the volume phase transition of microgels at the interface can be thought of as a quasi-1D collapse.<sup>51,52</sup> Finally, the VPT showed a hysteresis between heating and cooling cycles not found in the bulk. These results indicate that the presence of an interface alters the energy balance responsible for the VPT as polymer chains exhibit a tendency to spread at the interface to reduce surface tension.

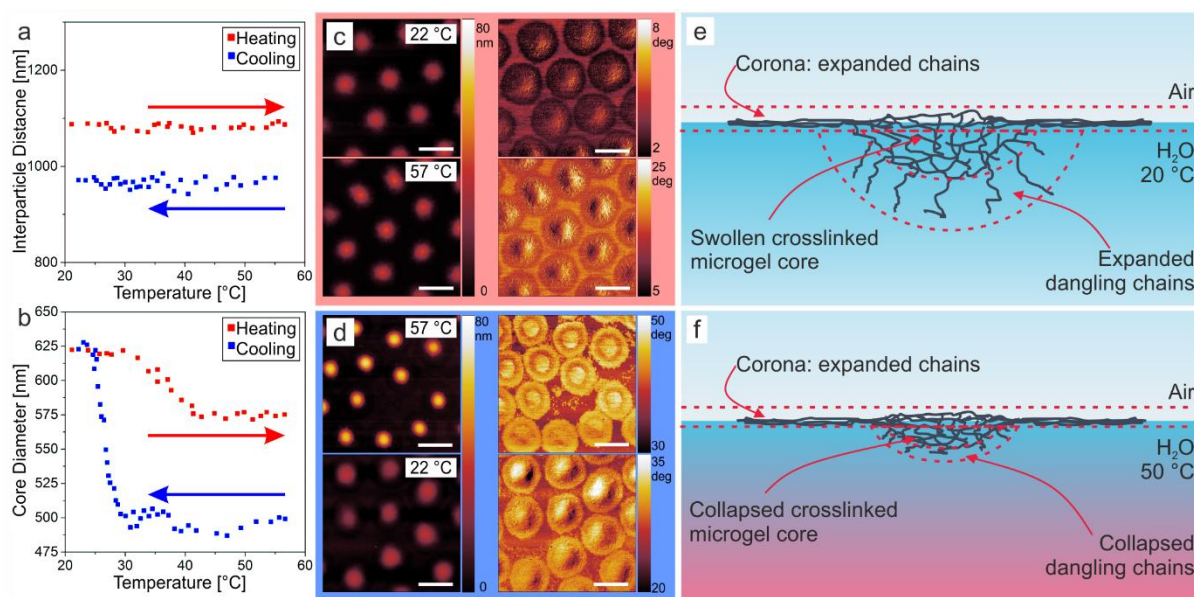


Figure 7: Volume phase transition of PNIPAM microgels adsorbed to the air/water interface at different subphase temperatures. a,b) Interparticle distance (a) and core diameter (b) – temperature diagram for heating (red) and cooling (blue). c,d) AFM height and phase images showing the “fried-egg” morphology even above the VPTT. Scale bar: 1  $\mu\text{m}$ . e-f) Schematic illustration of PNIPAM microgels adsorbed to the air/water below (e) and above (f) the VPTT. Adapted with permission from ref. 51. Copyright 2019 American Chemical Society.

### Complex and hierarchical interfacial assembly structures:

Typically, spherical particles interacting with an isotropic interaction potential self-assemble into hexagonal structures, when confined in two dimensions by a liquid interface. However, more complex patterns can be obtained by sequential deposition of microgel monolayers

(Figure 8).<sup>53-55</sup> In this approach, a hexagonal non-close packed microgel monolayer is deposited onto a substrate, followed by a second deposition of a similar microgel monolayer onto the same substrate. The obtained superstructure, formed by the organization of the two superimposed layers can be controlled by the applied drying conditions. Fast drying (<5 s) deposits the second monolayer on top of the first one, leading to the formation of a Moiré pattern (Figure 8b). During slow drying (5 min), the microgels of the second monolayer have sufficient mobility to find their equilibrium position in the interstitial sites of the first monolayer, leading to the formation of a lattice with honeycomb structure. The influence of the drying time is also captured by Brownian dynamics simulations using particles with a square shoulder potential (Figure 8d,e).

The same principle can be used to obtain binary alloys of large and small microgels. First, the large microgels are deposited on a solid substrate, followed by a deposition of the small microgels. During the second deposition of smaller microgels, the larger microgels, already fixed onto the substrate, reswell upon immersion into the water subphase and protrude the oil/water interface, thus interfering with the assembly of the smaller microgels. The smaller microgels thus assemble into the interstitial sites around the larger microgels (Figure 8Figuref). The obtained assembly further depends on the packing density of the second monolayer (Figure 8g). Additionally, these microgel patterns can be used as masks for metal-assisted chemical etching of silicon nanowires,<sup>26,46,53,56</sup> where the hierarchical structures show interesting anti-reflective properties in the visible range (Figure 8Figureh,i).<sup>53</sup>

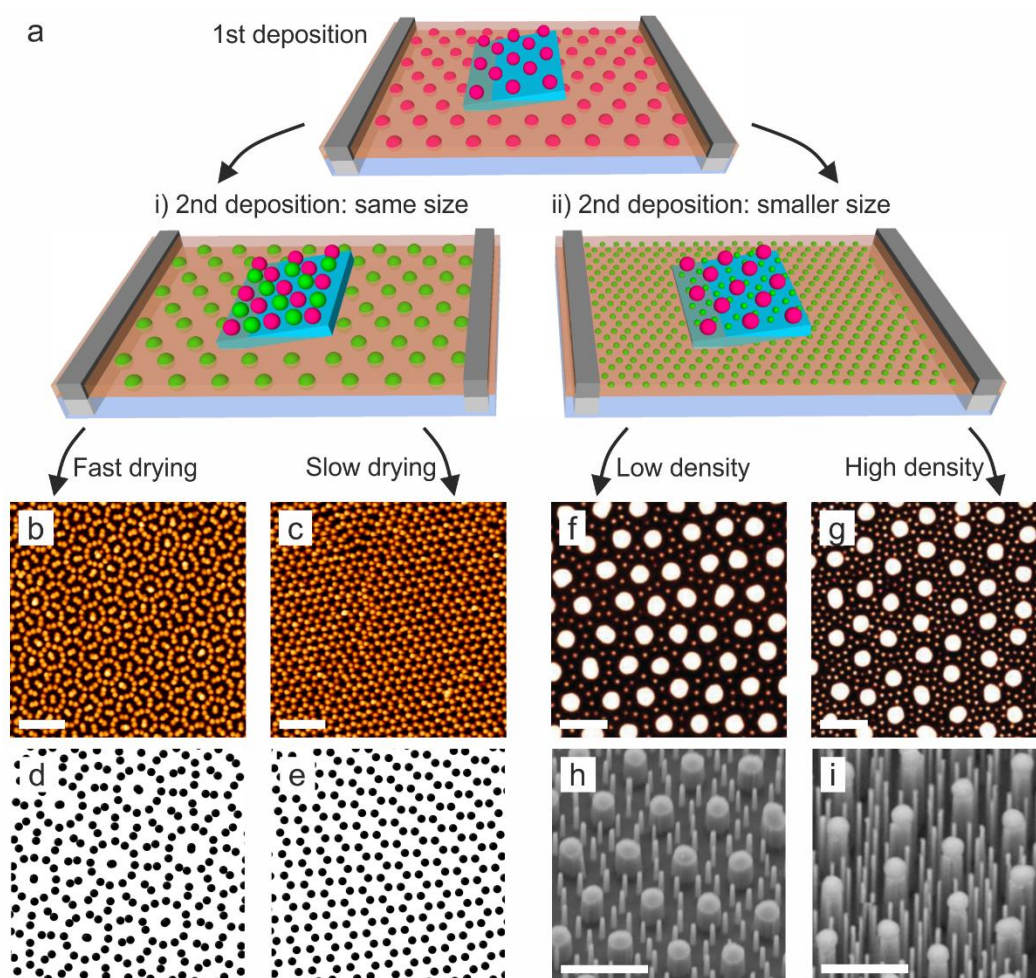


Figure 8: Complex surface patterning by sequential microgel monolayer deposition. a) Schematic illustration. While fast drying of two similar monolayers leads to Moiré pattern (b), slow drying leads to honeycomb structures (c). d,e) Brownian dynamics simulations reproduce both structures. Adapted with permission from ref. 54. Copyright 2019, the Royal Society of Chemistry. f-g) Sequential deposition of large and small microgels at low packing density (f) and high packing density (g) with subsequent silicon nanowire etching (h,i). Adapted with permission from ref. 53. Copyright 2018, the Royal Society of Chemistry. All scale bars: 2  $\mu\text{m}$ .

An alternative way to obtain complex self-assembled patterns is to modify the interaction potential of the colloidal particles interacting at the liquid interface. Non-hexagonal phases as minimum energy configurations have been predicted theoretically for isotropic particles interacting *via* a soft repulsive shoulder two decades ago.<sup>57</sup> The combination of a hard-sphere potential acting at the particle core with a longer range soft repulsion shoulder, known as Jagla potentials,<sup>57</sup> gives rise to a variety of different equilibrium structures at different surface

densities, including – counterintuitively for spherical building blocks – chains and square symmetries. The system minimizes its energy by fully overlapping the shells of neighboring particles in some directions in order to prevent the overlap of the shells in others.<sup>57,58</sup> These theoretically predicted phases have been recently experimentally realized using a mixed system of isotropic, spherical particles and soft, compressible microgels co-assembled at the air/water interface.<sup>59</sup> The attractive interactions between the two particle populations leads to the *in-situ* formation of a soft, compressible microgel corona around the polystyrene microspheres so that the binary system effectively acts as a one-component core-shell system with an increased repulsive character. Upon increasing the interfacial density of the particles, a complex phase diagram of assembly structures was observed, including chain and square phases, in agreement with minimum energy calculations and finite temperature Monte Carlo simulations of hard core-soft shoulder particles (Figure 9).<sup>59</sup>

These results underline the importance of interaction potentials on self-organization processes, demonstrating that surprising structural complexity can arise from the simplest possible building blocks. Recently, even more complex structural motifs including quasicrystalline order have been predicted *via* similar potentials,<sup>60,61</sup> which challenges experimentalists to further engineer the interaction potential of the involved colloidal particles.



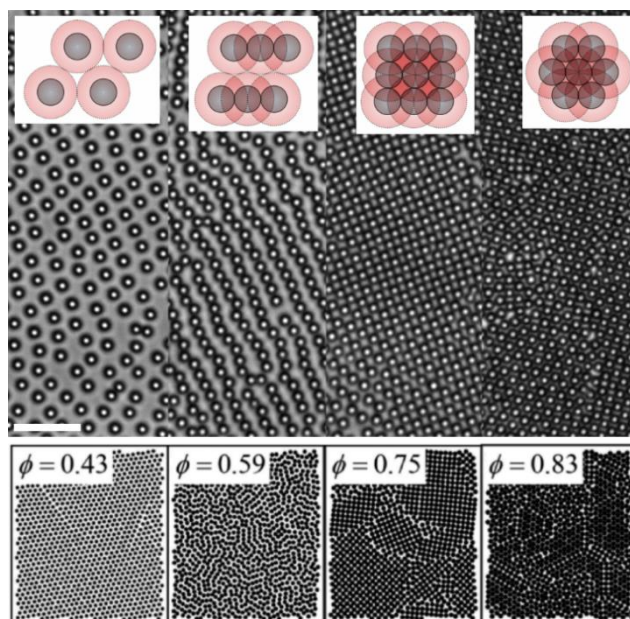


Figure 9: Complex self-assembly of mixtures of compressible microgels with polystyrene colloidal particles, effectively forming a core-shell system with a microgel corona separating the colloidal particles at the air/water interface. A complex phase diagram emerges upon changes of the interfacial density, including chains and square packing in addition to the known hexagonal close and non-close packing (top row), in agreement with Monte Carlo simulations of core-shell particles with a linear ramp potential (bottom row). Adapted with permission from ref. 59 .Copyright 2017 American Chemical Society. Scale bar: 10  $\mu\text{m}$ .

## Conclusion and Perspectives

In this review, we introduced fundamental concepts and important parameters to understand and control the interfacial behavior of nanogels and microgels. The interfacial properties of such soft objects are predominantly governed by their deformability and the presence of a thin corona surrounding the microgel core. The ability of these elements to at least partially deform and overlap upon compression leads to a more complex phase behavior compared to rigid particles. To further expand the understanding of this emerging soft particle system, several important challenges need to be addressed. A more detailed understanding of how the internal structure governs the interfacial morphology and phase behavior requires systematic investigations of defined microgel systems, for example with particularly uniform crosslinking densities,<sup>62</sup> with more complex structures such as hollow shells,<sup>63</sup> and with defined dangling chain structure to control the structure and dimensions of the interfacial

corona. Several fundamental questions need to be resolved concerning the structure of the corona in interacting microgel systems. To this point, it remains unclear whether microgel coronae overlap, entangle and intermix at the interface and how such interactions may be controlled. Computer models, now available for the accurate description of the interfacial properties of individual microgels, need to be expanded to capture interactions and phase behavior under compression. The engineering of interaction potential by combining soft and rigid interfacial elements, shown capable of forming non-intuitive assembly phases described by Jagla potentials, is still in its infancy but may be a promising avenue to realize even more complex assembly structures including quasi-crystalline phases. Finally, with the advancement of understanding of these fundamental interfacial properties, systems with tailored properties may further enhance the functional performance of microgels as innovative elements for the realization of future materials, such as tunable templates for surface patterning and coatings or responsive and compliant stabilizers for emulsions, foams, and liquid marbles.

## **AUTHOR INFORMATION**

### **Corresponding author**

\*nicolas.vogel@fau.de,

\*marcel.rey@fau.de

### **Author Contributions**

The manuscript was written through contributions of all authors. All authors have given approval to the final version of the manuscript.

### **Notes**

The authors declare no competing financial interest.

## **Biographies**

**Marcel Rey** received his Bachelor's and Master's degree in Material Science at the Eidgenössische Technische Hochschule (ETH) Zürich in 2015. He is currently a PhD student at the Friedrich-Alexander Universität (FAU) Erlangen-Nürnberg. His research focuses on soft particles at liquid interfaces.

**Miguel-Angel Fernandez-Rodriguez** received his Bachelor in Physics, Master degree in Colloids and Interfaces Science and Technology, and PhD in Physics at the University of Granada (Spain) in 2015. He is currently PostDoc researcher at ETH-Zurich. His research focuses on soft and Janus particles with interfacial activity, soft colloidal lithography and active matter.

**Matthias Karg** finished his studies of chemistry at the Technical University Berlin (Germany) in 2006. In 2009 he obtained his Ph.D. in physical chemistry from the same university. After a postdoctoral research stay at the Nanoscience Laboratory of the University of Melbourne (Australia) as a fellow of the Alexander von Humboldt foundation, he moved to the University of Bayreuth where he became junior professor in Physical Chemistry in 2012. Since 2016 he is full professor in the institute of Physical Chemistry I: Colloids and nanooptics at the Heinrich-Heine-University Düsseldorf, Germany. His current research interests include general aspects of colloid and interfaces science with a special focus on soft matter systems and plasmonic materials.

**Lucio Isa** received his Master's degree in Nuclear Engineering in 2004 from the Milan Polytechnic (Italy) and went on to obtain a PhD in Soft Condensed Matter in Physics at the University of Edinburgh (UK) in 2008. He then moved to ETH Zurich as a Marie-Curie Fellow, Swiss National Science Foundation (SNSF) Ambizione Fellow, SNSF Assistant



Professor and since 2019 is the ETH Zurich Professor of Soft Materials and Interfaces. His research tackles a broad class of materials and phenomena, with an emphasis on the behavior of colloids at interfaces and on the development of new active materials.

**Nicolas Vogel** studied chemistry at the Johannes-Gutenberg-University in Mainz (Germany) and Seoul National University (Republic of Korea) until 2008. In 2011, he received his PhD at the Max Planck Institute for Polymer Research in Mainz. After a postdoctoral research stay at the School of Engineering and Applied Sciences at Harvard University (USA), he was appointed associate professor in the Department of Chemical and Biological Engineering at the Friedrich-Alexander-University Erlangen-Nürnberg (Germany). He likes to apply self-assembly concepts to create materials with emergent functionalities.

### **Acknowledgments**

The research was supported by the Deutsche Forschungsgemeinschaft (DFG) under grant number VO 1824/8-1. N.V. also acknowledges support by the Interdisciplinary Center for Functional Particle Systems (FPS). M.A.F.R. and L.I. acknowledge the financial support of the Swiss National Science Foundation grant no. PP00P2 172913/1. M.K. acknowledges financial support through the Emmy Noether programme of the Deutsche Forschungsgemeinschaft (DFG, grant no. KA3880/1-1).

### **References:**

- (1) McGorty, R.; Fung, J.; Kaz, D.; Manoharan, V. N. Colloidal Self-Assembly at an Interface. *Mater. Today* **2010**, *13*, 34–42.
- (2) Binks, B. P.; Horozov, T. S. Aqueous Foams Stabilized Solely by Silica Nanoparticles. *Angew. Chemie - Int. Ed.* **2005**, *44*, 3722–3725.
- (3) Ramsden, W. Separation of Solids in the Surface-Layers of Solutions and “Suspensions” (Observations on Surface-Membranes, Bubbles, Emulsions, and Mechanical Coagulation). *Proc. R. Soc. London* **1903**, *72*, 156–164.
- (4) Pickering, S. U. Emulsions. *J. Chem. Soc., Trans.* **1907**, *91*, 2001–2021.

- (5) Pieranski, P. Two-Dimensional Interfacial Colloidal Crystals. *Phys. Rev. Lett.* **1980**, *45*, 569–572.
- (6) Kaz, D. M.; McGorty, R.; Mani, M.; Brenner, M. P.; Manoharan, V. N. Physical Ageing of the Contact Line on Colloidal Particles at Liquid Interfaces. *Nat. Mater.* **2011**, *11*, 138–142.
- (7) Grzelczak, M.; Vermant, J.; Furst, E. M.; Liz-Marzán, L. M. Directed Self-Assembly of Nanoparticles. *ACS Nano* **2010**, *4*, 3591–3605.
- (8) Vogel, N.; Retsch, M.; Fustin, C. A.; Del Campo, A.; Jonas, U. Advances in Colloidal Assembly: The Design of Structure and Hierarchy in Two and Three Dimensions. *Chem. Rev.* **2015**, *115*, 6265–6311.
- (9) Isa, L.; Buttinoni, I.; Fernandez-Rodriguez, M. A.; Vasudevan, S. A. Two-Dimensional Assemblies of Soft Repulsive Colloids Confined at Fluid Interfaces. *Epl* **2017**, *119*, 0–7.
- (10) Karg, M.; Pich, A.; Hellweg, T.; Hoare, T.; Lyon, L. A.; Crassous, J. J.; Suzuki, D.; Gumerov, R. A.; Schneider, S.; Potemkin, I. I.; Richtering, W. Nanogels and Microgels: From Model Colloids to Applications, Recent Developments and Future Trends. *Langmuir* **2019**, *35*, 6231–6255.
- (11) Pelton, R. H.; Chibante, P. Preparation of Aqueous Latices with N-Isopropylacrylamide. *Colloids and Surfaces* **1986**, *20*, 247–256.
- (12) Von Nessen, K.; Karg, M.; Hellweg, T. Thermoresponsive Poly-(N-Isopropylmethacrylamide) Microgels: Tailoring Particle Size by Interfacial Tension Control. *Polym. (United Kingdom)* **2013**, *54*, 5499–5510.
- (13) Sierra-Martin, B.; Retama, J. R.; Laurenti, M.; Fernández Barbero, A.; López Cabarcos, E. Structure and Polymer Dynamics within PNIPAM-Based Microgel Particles. *Adv. Colloid Interface Sci.* **2014**, *205*, 113–123.
- (14) Plamper, F. A.; Richtering, W. Functional Microgels and Microgel Systems. *Acc. Chem. Res.* **2017**, *50*, 131–140.
- (15) McPhee, W.; Tam, K. C.; Pelton, R. Poly(N-Isopropylacrylamide) Latices Prepared with Sodium Dodecyl Sulfate. *Journal of Colloid And Interface Science.* 1993, pp 24–30.
- (16) Kratz, K.; Hellweg, T.; Eimer, W. Rumah Susun Ramah Lansia. *Colloids Surfaces A Physicochem. Eng. Asp.* **2000**, *170*, 137–149.
- (17) Geisel, K.; Isa, L.; Richtering, W. The Compressibility of Ph-Sensitive Microgels at the Oil-Water Interface: Higher Charge Leads to Less Repulsion. *Angew. Chemie - Int. Ed.* **2014**, *53*, 4905–4909.
- (18) Wu, X.; Pelton, R. H.; Hamielec, A. E.; Woods, D. R.; McPhee, W. The Kinetics of Poly(N-Isopropylacrylamide) Microgel Latex Formation. *Colloid Polym. Sci.* **1994**, *272*, 467–477.
- (19) Fernández-Barbero, A.; Fernández-Nieves, A.; Grillo, I.; López-Cabarcos, E. Structural Modifications in the Swelling of Inhomogeneous Microgels by Light and Neutron Scattering. *Phys. Rev. E - Stat. Nonlinear, Soft Matter Phys.* **2002**, *66*, 1–10.
- (20) Acciaro, R.; Gilanyi, T.; Varga, I. Preparation of Monodisperse Poly(N-Isopropylacrylamide) Microgel Particles with Homogenous Cross-Link Density

- Distribution. *Langmuir* **2011**, *27*, 7917–7925.
- (21) Landfester, K.; Musyanovych, A. *Hydrogels in Miniemulsions*; Springer, Berlin, Heidelberg, 2010.
  - (22) Minato, H.; Murai, M.; Watanabe, T.; Matsui, S.; Takizawa, M.; Kureha, T.; Suzuki, D. The Deformation of Hydrogel Microspheres at the Air/Water Interface. *Chem. Commun.* **2018**, *54*, 932–935.
  - (23) Destribats, M.; Lapeyre, V.; Wolfs, M.; Sellier, E.; Leal-Calderon, F.; Ravaine, V.; Schmitt, V. Soft Microgels as Pickering Emulsion Stabilisers: Role of Particle Deformability. *Soft Matter* **2011**, *7*, 7689–7698.
  - (24) Pinaud, F.; Geisel, K.; Massé, P.; Catargi, B.; Isa, L.; Richtering, W.; Ravaine, V.; Schmitt, V. Adsorption of Microgels at an Oil-Water Interface: Correlation between Packing and 2D Elasticity. *Soft Matter* **2014**, *10*, 6963–6974.
  - (25) Geisel, K.; Isa, L.; Richtering, W. Unraveling the 3D Localization and Deformation of Responsive Microgels at Oil/Water Interfaces: A Step Forward in Understanding Soft Emulsion Stabilizers. *Langmuir* **2012**, *28*, 15770–15776.
  - (26) Scheidegger, L.; Fernández-Rodríguez, M. Á.; Geisel, K.; Zanini, M.; Elnathan, R.; Richtering, W.; Isa, L. Compression and Deposition of Microgel Monolayers from Fluid Interfaces: Particle Size Effects on Interface Microstructure and Nanolithography. *Phys. Chem. Chem. Phys.* **2017**, *19*, 8671–8680.
  - (27) Style, R. W.; Isa, L.; Dufresne, E. R. Adsorption of Soft Particles at Fluid Interfaces. *Soft Matter* **2015**, *11*, 1–8.
  - (28) Camerin, F.; Fernández-Rodríguez, M. Á.; Rovigatti, L.; Antonopoulou, M.-N.; Gnan, N.; Ninarello, A.; Isa, L.; Zaccarelli, E. Microgels Adsorbed at Liquid–Liquid Interfaces: A Joint Numerical and Experimental Study. *ACS Nano* **2019**, *13*, 4548–4559.
  - (29) Zielińska, K.; Sun, H.; Campbell, R. A.; Zorbakhsh, A.; Resmini, M. Smart Nanogels at the Air/Water Interface: Structural Studies by Neutron Reflectivity. *Nanoscale* **2016**, *8*, 4951–4960.
  - (30) Rumyantsev, A. M.; Gumerov, R. A.; Potemkin, I. I. A Polymer Microgel at a Liquid-Liquid Interface: Theory: Vs. Computer Simulations. *Soft Matter* **2016**, *12*, 6799–6811.
  - (31) Mehrabian, H.; Harting, J.; Snoeijer, J. H. Soft Particles at a Fluid Interface. *Soft Matter* **2015**, *12*, 1–17.
  - (32) Gnan, N.; Rovigatti, L.; Bergman, M.; Zaccarelli, E. In Silico Synthesis of Microgel Particles. *Macromolecules* **2017**, *50*, 8777–8786.
  - (33) Ninarello, A.; Crassous, J. J.; Paloli, D.; Camerin, F.; Gnan, N.; Rovigatti, L.; Schurtenberger, P.; Zaccarelli, E. Advanced Modelling of Microgel Structure across the Volume Phase Transition. *arXiv Prepr. arXiv* **2019**, 1901.11495.
  - (34) Schmidt, S.; Liu, T.; Rütten, S.; Phan, K. H.; Möller, M.; Richtering, W. Influence of Microgel Architecture and Oil Polarity on Stabilization of Emulsions by Stimuli-Sensitive Core-Shell Poly(N -Isopropylacrylamide- Co -Methacrylic Acid) Microgels: Mlickering versus Pickering Behavior? *Langmuir* **2011**, *27*, 9801–9806.
  - (35) Rey, M.; Hou, X.; Tang, J. S. J.; Vogel, N. Interfacial Arrangement and Phase Transitions of PNIPAm Microgels with Different Crosslinking Density. *Soft Matter*

2017, 13, 8717–8727.

- (36) Geisel, K.; Richtering, W.; Isa, L. Highly Ordered 2D Microgel Arrays: Compression versus Self-Assembly. *Soft Matter* **2014**, *10*, 7968.
- (37) Rey, M.; Fernández-Rodríguez, M. Á.; Steinacher, M.; Scheidegger, L.; Geisel, K.; Richtering, W.; Squires, T. M.; Isa, L. Isostructural Solid–Solid Phase Transition in Monolayers of Soft Core–Shell Particles at Fluid Interfaces: Structure and Mechanics. *Soft Matter* **2016**, *12*, 3545–3557.
- (38) Picard, C.; Garrigue, P.; Tatry, M. C.; Lapeyre, V.; Ravaine, S.; Schmitt, V.; Ravaine, V. Organization of Microgels at the Air – Water Interface under Compression: Role of Electrostatics and Cross-Linking Density. *Langmuir* **2017**, *33*, 7968–7981.
- (39) Rauh, A.; Rey, M.; Barbera, L.; Zanini, M.; Karg, M.; Isa, L. Compression of Hard Core–Soft Shell Nanoparticles at Liquid–Liquid Interfaces: Influence of the Shell Thickness. *Soft Matter* **2017**, *13*, 158–169.
- (40) Gavrilov, A. A.; Richtering, W.; Potemkin, I. I. Polyelectrolyte Microgels at a Liquid–Liquid Interface: Swelling and Long-Range Ordering. *J. Phys. Chem. B* **2019**, *123*, 8590–8598.
- (41) Scotti, A.; Bochenek, S.; Brugnoli, M.; Fernandez-Rodriguez, M. A.; Schulte, M. F.; Houston, J. E.; Gelissen, A. P. H.; Potemkin, I. I.; Isa, L.; Richtering, W. Exploring the Colloid-to-Polymer Transition for Ultra-Low Crosslinked Microgels from Three to Two Dimensions. *Nat. Commun.* **2019**, *10*, 1418.
- (42) Karg, M.; Pastoriza-Santos, I.; Liz-Marzán, L. M.; Hellweg, T. A Versatile Approach for the Preparation of Thermosensitive PNIPAM Core-Shell Microgels with Nanoparticle Cores. *ChemPhysChem* **2006**, *7*, 2298–2301.
- (43) Karg, M.; Wellert, S.; Prevost, S.; Schweins, R.; Dewhurst, C.; Liz-Marzán, L. M.; Hellweg, T. Well Defined Hybrid PNIPAM Core-Shell Microgels: Size Variation of the Silica Nanoparticle Core. *Colloid Polym. Sci.* **2011**, *289*, 699–709.
- (44) Vasudevan, S. A.; Rauh, A.; Barbera, L.; Karg, M.; Isa, L. Stable in Bulk and Aggregating at the Interface: Comparing Core-Shell Nanoparticles in Suspension and at Fluid Interfaces. *Langmuir* **2018**, *34*, 886–895.
- (45) Vogel, N.; Fernández-López, C.; Pérez-Juste, J.; Liz-Marzán, L. M.; Landfester, K.; Weiss, C. K. Ordered Arrays of Gold Nanostructures from Interfacially Assembled Au@ PNIPAM Hybrid Nanoparticles. *Langmuir* **2012**, *28*, 8985–8993.
- (46) Tang, J. S. J.; Bader, R. S.; Goerlitzer, E. S. A.; Wendisch, J. F.; Bourret, G. R.; Rey, M.; Vogel, N. Surface Patterning with SiO<sub>2</sub>@PNiPAm Core–Shell Particles. *ACS Omega* **2018**, *3*, 12089–12098.
- (47) Vasudevan, S. A.; Rauh, A.; Kröger, M.; Karg, M.; Isa, L. Dynamics and Wetting Behavior of Soft Particles at a Fluid-Fluid Interface. *Langmuir* **2018**, *34*, 15370–15382.
- (48) Richtering, W. Responsive Emulsions Stabilized by Stimuli-Sensitive Microgels: Emulsions with Special Non-Pickering Properties. *Langmuir* **2012**, *28*, 17218–17229.
- (49) Li, Z.; Ngai, T. Microgel Particles at the Fluid-Fluid Interfaces. *Nanoscale* **2013**, *5*, 1399–1410.
- (50) Schmitt, V.; Ravaine, V. Surface Compaction versus Stretching in Pickering Emulsions Stabilised by Microgels. *Curr. Opin. Colloid Interface Sci.* **2013**, *18*, 532–541.

- (51) Harrer, J.; Rey, M.; Ciarella, S.; Löwen, H.; Janssen, L. M. C.; Vogel, N. Stimuli-Responsive Behavior of PNIPAm Microgels under Interfacial Confinement. *Langmuir* **2019**, *35*, 10512–10521.
- (52) Bochenek, S.; Scotti, A.; Ogieglo, W.; Fernandez-Rodriguez, M. A.; Schulte, M. F.; Gumerov, R. A.; Bushuev, N. V.; Potemkin, I. I.; Wessling, M.; Isa, L.; Richtering, W. Effect of the 3D Swelling of Microgels on Their 2D Phase Behavior at the Liquid-Liquid Interface. **2019**.
- (53) Fernandez-Rodriguez, M. A.; Elnathan, R.; Ditcovski, R.; Grillo, F.; Conley, G. M.; Timpu, F.; Rauh, A.; Geisel, K.; Ellenbogen, T.; Grange, R.; Scheffold, F.; Karg, M.; Richtering, W.; Voelcker, N. H.; Isa, L. Tunable 2D Binary Colloidal Alloys for Soft Nanotemplating. *Nanoscale* **2018**, *10*, 22189–22195.
- (54) Volk, K.; Deißbeck, F.; Mandal, S.; Löwen, H.; Karg, M. Moiré and Honeycomb Lattices through Self-Assembly of Hard-Core/Soft-Shell Microgels: Experiment and Simulation. *Phys. Chem. Chem. Phys.* **2019**, *21*, 19153–19162.
- (55) Grillo, F.; Fernandez-Rodriguez, M.-A.; Antonopoulou, M.-N.; Gerber, D.; Isa, L. Self-Templating Assembly of Soft Microparticles into Complex Tessellations. *arXiv Prepr. arXiv1911.13171*. **2019**, 1–9.
- (56) Rey, M.; Elnathan, R.; Ditcovski, R.; Geisel, K.; Zanini, M.; Fernandez-Rodriguez, M. A.; Naik, V. V.; Frutiger, A.; Richtering, W.; Ellenbogen, T.; Voelcker, N. H.; Isa, L. Fully Tunable Silicon Nanowire Arrays Fabricated by Soft Nanoparticle Templating. *Nano Lett.* **2016**, *16*, 157–163.
- (57) Jagla, E. A. Phase Behavior of a System of Particles with Core Collapse. *Phys. Rev. E* **1998**, *58*, 11.
- (58) Malescio, G.; Pellicane, G. Stripe Phases from Isotropic Repulsive Interactions. *Nat. Mater.* **2003**, *2*, 97–100.
- (59) Rey, M.; Law, A. D.; Buzza, D. M. A.; Vogel, N. Anisotropic Self-Assembly from Isotropic Colloidal Building Blocks. *J. Am. Chem. Soc.* **2017**, *139*, 17464–17473.
- (60) Dotera, T.; Oshiro, T.; Zihlerl, P. Mosaic Two-Lengthscale Quasicrystals. *Nature* **2014**, *506*, 208–211.
- (61) Kryuchkov, N. P.; Yurchenko, S. O.; Fomin, Y. D.; Tsiok, E. N.; Ryzhov, V. N. Complex Crystalline Structures in a Two-Dimensional Core-Softened System. *Soft Matter* **2018**, *14*, 2152–2162.
- (62) Still, T.; Chen, K.; Alsayed, A. M.; Aptowicz, K. B.; Yodh, A. G. Synthesis of Micrometer-Size Poly(N-Isopropylacrylamide) Microgel Particles with Homogeneous Crosslinker Density and Diameter Control. *J. Colloid Interface Sci.* **2013**, *405*, 96–102.
- (63) Geisel, K.; Rudov, A. A.; Potemkin, I. I.; Richtering, W. Hollow and Core-Shell Microgels at Oil-Water Interfaces: Spreading of Soft Particles Reduces the Compressibility of the Monolayer. *Langmuir* **2015**, *31*, 13145–13154.